Morbillivirus control of the interferon response: relevance of STAT2 and mda5 but not STAT1 for canine distemper virus virulence in ferrets.

Nicholas Svitek, Ingo Gerhauser, Christophe Goncalves, Elena Grabski, Marius Döring, Ulrich Kalinke, Danielle E Anderson, Roberto Cattaneo, Veronika von Messling

JVI Journals.ASM.org

Morbillivirus Control of the Interferon Response: Relevance of STAT2 and mda5 but Not STAT1 for Canine Distemper Virus Virulence in Ferrets

Nicholas Svitek,[a] Ingo Gerhauser,[b,c] Christophe Goncalves,[a] Elena Grabski,[d] Marius Döring,[d] Ulrich Kalinke,[d] Danielle E. Anderson,[b] Roberto Cattaneo,[e] Veronika von Messling[a,b,f]

INRS-Institut Armand-Frappier, University of Quebec, Laval, Quebec, Canada[a]; Emerging Infectious Diseases Program, Duke-NUS Graduate Medical School Singapore, Singapore, Republic of Singapore[b]; Department of Pathology, University of Veterinary Medicine, Hannover, Germany[c]; Institute for Experimental Infection Research, TWINCORE, Centre for Experimental and Clinical Infection Research, Helmholtz-Centre for Infection Research (HZI) and Hannover Medical School (MHH), Hannover, Germany[d]; Department of Molecular Medicine and Virology and Gene Therapy Graduate Track, Mayo Clinic College of Medicine, Rochester, Minnesota, USA[e]; Veterinary Medicine Division, Paul-Ehrlich-Institute, Federal Institute for Vaccines and Biomedicines, Langen, Germany[f]

ABSTRACT

The V proteins of paramyxoviruses control the innate immune response. In particular, the V protein of the genus *Morbillivirus* interferes with the signal transducer and activator of transcription 1 (STAT1), STAT2, and melanoma differentiation-associated protein 5 (mda5) signaling pathways. To characterize the contributions of these pathways to canine distemper virus (CDV) pathogenesis, we took advantage of the knowledge about the mechanisms of interaction between the measles virus V protein with these key regulators of innate immunity. We generated recombinant CDVs with V proteins unable to properly interact with STAT1, STAT2, or mda5. A virus with combined STAT2 and mda5 deficiencies was also generated, and available wild-type and V-protein-knockout viruses were used as controls. Ferrets infected with wild-type and STAT1-blind viruses developed severe leukopenia and loss of lymphocyte proliferation activity and succumbed to the disease within 14 days. In contrast, animals infected with viruses with STAT2 or mda5 defect or both STAT2 and mda5 defects developed a mild self-limiting disease similar to that associated with the V-knockout virus. This study demonstrates the importance of interference with STAT2 and mda5 signaling for CDV immune evasion and provides a starting point for the development of morbillivirus vectors with reduced immunosuppressive properties.

IMPORTANCE

The V proteins of paramyxoviruses interfere with the recognition of the virus by the immune system of the host. For morbilliviruses, the V protein is known to interact with the signal transducer and activator of transcription 1 (STAT1) and STAT2 and the melanoma differentiation-associated protein 5 (mda5), which are involved in interferon signaling. Here, we examined the contribution of each of these signaling pathways to the pathogenesis of the carnivore morbillivirus canine distemper virus. Using viruses selectively unable to interfere with the respective signaling pathway to infect ferrets, we found that inhibition of STAT2 and mda5 signaling was critical for lethal disease. Our findings provide new insights in the mechanisms of morbillivirus immune evasion and may lead to the development of new vaccines and oncolytic vectors.

Morbilliviruses, including measles virus (MeV), which infects humans and certain nonhuman primates, and the carnivore morbillivirus canine distemper virus (CDV), cause a severe acute disease characterized by rash, fever, and respiratory and gastrointestinal symptoms, followed by generalized immunosuppression (1–3). This rapid and profound immunosuppression facilitates secondary infections, which make important contributions to morbillivirus-associated morbidity and mortality (4, 5). The morbillivirus V protein is the primary viral immune interference protein, targeting the innate host response at multiple levels (6–8). The V-protein mRNA is transcribed from the phosphoprotein (P) gene by insertion of a nontemplated guanosine at an editing site located in the middle of the gene (9, 10). Consequently, V shares its amino-terminal part with P, but has a unique carboxy terminus. The latter contains a cysteine-rich domain, which binds two atoms of zinc (11, 12) and is highly conserved among morbilliviruses and other paramyxoviruses (13).

The shared amino-terminal domain and the unique carboxyl-terminal domain contribute to the innate immunity-interfering functions of morbillivirus V protein. The P/V shared domain alone can block type I and type II interferon (IFN) responses. This activity has been mapped to amino acids 110 to 130, with tyrosine 110 being essential for binding the signal transducer and activator of transcription 1 (STAT1) molecule (14–16). Inactivation of the zinc-binding domains in the V-protein unique region results in a 70% loss of its type I IFN inhibitory activity (8), and this region can directly inhibit beta interferon (IFN-β) synthesis by interacting with the double-stranded RNA sensor melanoma differentiation-associated gene 5 (mda5) (7, 17, 18). Systematic mutagenesis of the entire region revealed that aspartic acid at position 248 and,

Received 19 October 2013 **Accepted** 19 December 2013
Published ahead of print 26 December 2013
Editor: T. S. Dermody
Address correspondence to Veronika von Messling, veronika.vonmessling@pei.de.
N.S. and I.G. contributed equally to this study.

doi:10.1128/JVI.03076-13

to a lesser extent, phenylalanine 246 are important for the inhibition of STAT2 nuclear translocation (6, 8). Similarly, it was demonstrated that a conserved arginine at position 235 is required for mda5 interference in several paramyxoviruses (19). The STAT2 and mda5 interaction sites of the MeV carboxyl-terminal domain are thus located at opposite sides of the first zinc-binding domain, which is formed between histidine at position 232 and the first conserved cysteine at position 251.

Relevance of morbillivirus V proteins for virulence has been demonstrated in different susceptible hosts. Rhesus macaques infected with a V-knockout (Vko) wild-type MeV experienced shorter viremia and less immunosuppression (20), and infection with a STAT1blind virus resulted in a similar phenotype (21). In ferrets, a Vko derivative of a lethal wild-type CDV strain caused only a very mild disease and no longer triggered the inhibition of lymphocyte proliferation upon nonspecific stimulation that is indicative of immunosuppression (22). To assess the contributions of the different V-protein interactions to the control of innate immunity, we first validated the residues involved in V-protein interactions with STAT2 and mda5 in the CDV context. A panel of STAT1-, STAT2-, mda5-, and combined STAT2/mda5-blind derivatives of the 5804P wild-type CDV strain was generated, and their growth phenotypes were characterized *in vitro*. The virulence and extent of immunosuppression were then assessed in ferrets, and the extent of IFN induction was quantified.

MATERIALS AND METHODS

Cells and viruses. VerodogSLAMtag cells (23) and Huh7 cells (JCRB0403) were maintained in Dulbecco's modified Eagle's medium (Life Technologies, Burlington, ON, Canada) with 5% fetal bovine serum (Life Technologies). CDV strains 5804PeH (24) and 5804PeH Vko (22), and all recombinant viruses produced were grown in VerodogSLAMtag cells.

Luciferase reporter gene assays. The 5804P V gene was cloned into the mammalian expression plasmid pCG, and the respective mutations and the individual mutations W246G, I247L, D248Y, and K249E were introduced by site-directed mutagenesis. For each V-protein mutant, triplicate wells of Huh7 cells seeded in black 96-well plates (Greiner Bio-One, Monroe, NC, USA) were transfected using Lipofectamine 2000 (Invitrogen, Burlington, ON, Canada) with 0.08 μg of the respective V-gene expression plasmid or empty vector control, 0.04 μg of pRL-TK (Promega, Madison, WI, USA) as an internal control for transfection efficiency, and 0.08 μg of either pISRE-Luc (Luc stands for luciferase) (Stratagene, La Jolla, CA, USA) to assess type I IFN-mediated transcriptional activation, pGAS-luc (Stratagene) for IFN-γ-mediated activation, or p125-luc together with mda5 or RIG-I (retinoic acid-inducible gene I product) expression plasmids for IFN-β promoter activation. At 40 h after pISRE-Luc transfection, the medium was replaced with fresh medium supplemented with 1,000 U/ml of universal type I IFN-α (PBL Interferon Source, Piscataway, NJ, USA). To assess pGAS-luc-mediated or IFN-β promoter activation, the medium was replaced 24 h after transfection with fresh medium supplemented with 100 ng/ml of human IFN-γ (PBL Interferon Source) or 1 μg/ml of poly(I·C) (LyoVec; InvivoGen, San Diego, CA, USA), respectively. Cells were harvested 8 h after IFN-α stimulation, 18 h after IFN-γ stimulation, or 20 h after poly(I·C) stimulation in Dual-Glo luciferase assay lysis buffer (Promega), and luciferase activity was measured using a luminometer (Infinite 200 PRO microplate reader; Tecan Asia Ptd. Ltd., Singapore). Values for firefly luciferase activity were normalized to *Renilla* luciferase activity, and results were expressed as a percentage of the empty vector control stimulated value. Each luciferase assay was performed at least three times.

Antibodies and indirect immunofluorescence. CDV V protein was detected with a polyclonal rabbit antipeptide serum raised against amino acids 18 to 39 of the shared P/V domain (25). STAT1 and STAT2 were detected using commercially available monoclonal antibodies (C-111 and A-7, respectively; Santa Cruz Biotechnology, Santa Cruz, CA, USA). Alexa Fluor 568-conjugated donkey anti-rabbit (Life Technologies) and Alexa Fluor 647-conjugated goat anti-mouse (Life Technologies) secondary antibodies were used. For immunofluorescence analysis, 4×10^4 Huh7 cells were grown in Nunc Lab-Tek II 8-chamber slide system (Thermo Fisher, Langenselbold, Germany) and transfected with 0.2 μg of empty vector or V-expressing plasmids using Lipofectamine 2000 according to the manufacturer's instructions. At 36 h posttransfection, cells were stimulated with 1,000 U/ml IFN-α2b (Essex Pharma GmbH, Munich, Germany) or 2,000 U/ml of human IFN-γ (Preprotech, Hamburg, Germany) for 30 min. The cells were then washed with phosphate-buffered saline (PBS) (Life Technologies), fixed with 4% paraformaldehyde in PBS for 10 min at room temperature, and permeabilized with 0.1% Triton X-100 in PBS for 5 min at 4°C. Samples were blocked with 2% fetal bovine serum for 1 h followed by sequential incubation with the respective primary and secondary antibodies for 45 min and 30 min at room temperature, respectively. Finally, cell nuclei were stained with 4′,6-diamidino-2-phenylindole (DAPI) for 1 min at room temperature. Images were obtained using a confocal microscope (Olympus FluoView 1000) during 405-nm, 561-nm, and 633-nm laser stimulation using an UOlanSApo 60×/1.35 oil objective. Colocalization was analyzed using the ImageJ software Intensity correlation analysis plugin (National Institutes of Health). Pearson's coefficients were calculated for every cell individually by manually defining the region of interest. Values −1 to 0 indicate no colocalization, values around zero represent random distribution (no correlation), and values 0 to 1 indicate colocalization. The higher the Pearson's coefficient, the stronger the degree of colocalization.

Western blot analysis. VerodogSLAMtag cells were plated at a density of 5×10^5 cells per well in a 6-well plate, infected with the respective viruses at a multiplicity of infection (MOI) of 0.1, and incubated at 37°C for 48 h. For the analysis of viral protein expression, cells were lysed in radioimmunoprecipitation assay (RIPA) buffer (1 mM phenylmethylsulfonyl fluoride, 1% sodium deoxycholate, 50 mM Tris-HCl [pH 7.4], 1% Triton X-100, 0.1% SDS, 150 mM NaCl), and proteins were separated by SDS-polyacrylamide gel electrophoresis followed by transfer to polyvinyl difluoride membranes (Merck Millipore, Billerica, MA, USA). P and V proteins were detected using the CDV P/V-specific rabbit antipeptide antiserum against the P/V shared domain (25) in combination with a peroxidase-coupled donkey anti-rabbit secondary antiserum and visualized using ECL Plus Western blotting detection system (GE Healthcare, Pittsburgh, PA, USA) and an ImageQuant LAS 4000 chemiluminescent image analyzer (GE Healthcare).

Generation of recombinant viruses. The mutations resulting in the amino acid substitution Y110H, E235A, WI246/7GL, and C255S (Fig. 1A) were introduced into a subcloned P gene fragment flanked by the unique restriction sites KpnI and SacII. The fragment was then transferred into the 5804PeH genomic cDNA containing the enhanced green fluorescent protein (eGFP) in an additional transcriptional unit between the hemagglutinin (H) and polymerase (L) genes. Recombinant viruses were recovered using the reverse genetics system described in reference 25. Briefly, 293 cells were transfected with expression plasmids encoding the MeV nucleoprotein (N), phosphoprotein (P), and polymerase (L) protein and the T7 polymerase, together with the respective genomic 5804PeH plasmid. Two days after transfection, the cells were transferred onto VerodogSLAMtag cells, and individual syncytia were picked and expanded on fresh VerodogSLAMtag cells to produce virus stocks. Virus titers were quantified by the limited dilution method and expressed as 50% tissue culture infectious doses ($TCID_{50}$).

Animal experiments and assessment of virulence. All animal experiments were approved by the INRS-Institut Armand-Frappier or SingHealth Institutional Animal Care and Use Committees. Groups of at least six CDV-seronegative male ferrets (*Mustela putorius furo*) were infected intranasally with 10^5 $TCID_{50}$ of each virus as described previously (22).

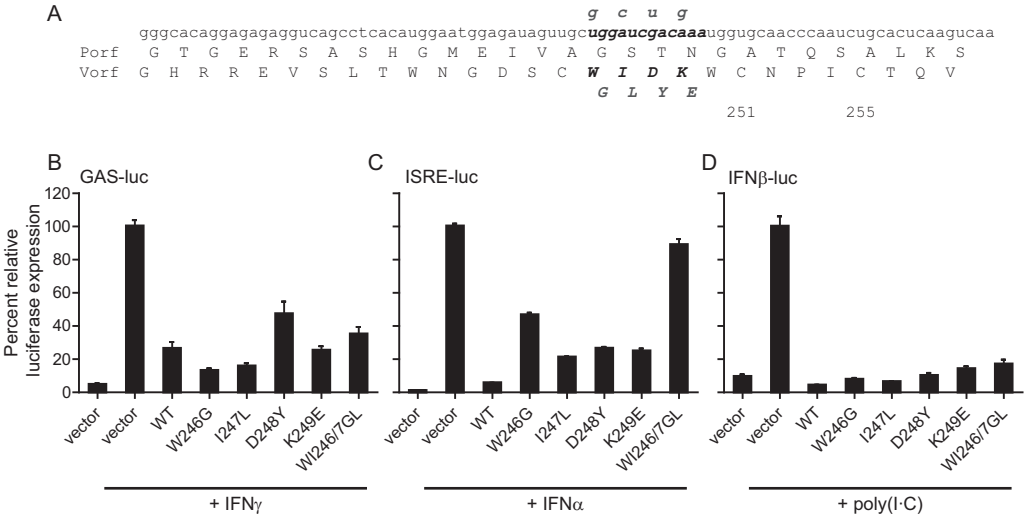

FIG 1 Characterization of a STAT2blind V protein without alteration of the P open reading frame (Porf). (A) Nucleotide and P- and V-protein sequences of the STAT2-binding region. STAT2-binding residues are indicated in boldface type, and the corresponding nucleotide sequence is shown in italic boldface type. Mutations that alter the V-protein sequence while maintaining the P-protein sequence are shown in gray. C245 is not conserved and may not be used to complex zinc. (B to D) IFN signaling interference activity of the V-protein mutants. Huh7 cells were transfected with either a GAS-luciferase reporter gene plasmid (B), ISRE-luciferase reporter gene plasmid (C), or IFN-β–luciferase reporter gene plasmid (D) in combination with either an empty vector, or vectors expressing the CDV wild-type (WT) V protein, or the respective mutant CDV V proteins as indicated. The cells were treated with 100 ng/ml of IFN-γ or 1,000 U/ml of IFN-α or transfected with 1 μg/ml of poly(I·C) for 18 h, 8 h, or 20 h prior to lysis, respectively, and luciferase activity was measured. Luciferase activity of cells transfected with an empty vector was set at 100%. Values are the averages of three experiments done in triplicate; error bars indicate the standard errors of the means (SEM).

Rash, fever, and weight loss were assessed daily and graded on a scale from 0 to 2 (scored as 0, 1, and 2). The total white blood cell count was determined from fresh EDTA-treated blood diluted 1:100 in 3% acetic acid, and the viremia and lymphocyte proliferation activity were quantified. Briefly, the erythrocytes in the EDTA-treated blood were lysed in ACK lysing buffer (Life Technologies). The white blood cells were then counted, and 10-fold dilution steps were transferred onto Verodog-SLAMtag cells. Titers were expressed as $TCID_{50}/10^6$ cells. At the last time point of virus detection in peripheral blood mononuclear cells (PBMCs), RNA was isolated from the remaining cells stored in RNAlater (Life Technologies), and the region of the P gene containing the mutation was amplified by reverse transcription-PCR (RT-PCR) and sequenced.

Ficoll (GE Healthcare) density gradient centrifugation was used to isolate PBMCs from heparinized blood. The proliferation of PBMCs after stimulation with 15 μg/ml of phytohemagglutinin (PHA) (Life Technologies) was quantified using a chemiluminescence immunoassay based on the measurement of 5-bromo-2′-deoxyuridine (BrdU) incorporation during DNA synthesis (Roche Applied Science, Indianapolis, IN). The *in vitro* proliferation activity was expressed as the ratio between PHA-stimulated and nonstimulated cells.

IFN mRNA analysis. Relative IFN-α, IFN-β, and IFN-γ mRNA levels were analyzed by semiquantitative real-time PCR analysis as described previously (26). Briefly, mRNA was isolated from PBMCs of infected ferrets using the RNeasy minikit (Qiagen, Mississauga, ON, Canada). Ten ng of RNA together with specific primers against ferret IFN-α, -β, or -γ was mixed with the QuantiTect SYBR green RT-PCR master mix (Qiagen) following the manufacturer's instructions. Glyceraldehyde-3-phosphate dehydrogenase (GAPDH) mRNA transcription was used as an internal control, and mRNA levels were normalized to day 0 values. The relative change in transcription levels was calculated using the formula fold change $= 2^{-\Delta\Delta Ct}$ to evaluate fold transcription (26, 27).

RESULTS

The STAT1, STAT2, and mda5 interaction sites in the V protein are conserved between MeV and CDV. Morbilliviruses interfere with IFN activation by preventing the nuclear translocation of STAT1 and STAT2 (28) as well as downstream signaling through the intracellular pattern recognition receptor mda5 (7, 29). The V-protein residues involved in these functions have been mapped for MeV (8, 19), and the importance of Y110H for STAT1 binding and the region for STAT2 and mda5 interactions has been demonstrated for other morbilliviruses (16, 30). To investigate the roles of the different signaling pathways in morbillivirus pathogenesis, we selectively generated STAT1-, STAT2-, or mda5-blind CDV V proteins and a V protein with a disrupted zinc-binding domain (ZBDko) in the genetic background of the wild-type strain 5804P.

To specifically abolish STAT2 binding while maintaining the P open reading frame, the combination of the two point mutations W246G and I247L in the STAT2-binding region covering residues 240 to 250 identified in MeV V (8) was required (Fig. 1A and 2A and B). The WI246/7GL protein was STAT2blind but continued to block STAT1 signaling and IFN-β promoter activation (Fig. 1B to D). To generate a STAT1blind derivative, the Y110H mutation was introduced into the P/V shared amino-terminal part of the V protein, and the E235A and C255S mutations were introduced into the V-protein unique region (Fig. 2B) to obtain the mda5 and ZBDko derivatives, respectively (Fig. 2A).

The interference of the parental V protein and the four mutant V proteins with IFN signaling activation was evaluated using luciferase reporter gene assays. After transfection in Huh7 cells, all V proteins were expressed at similar levels (data not shown). Reporter plasmids carrying firefly luciferase under the control of either the IFN-γ-activated sequence (GAS) to evaluate STAT1-mediated type II IFN signaling activation, repetitive sequences of the IFN-stimulated response element (ISRE) to evaluate STAT1/STAT2 heterodimer-dependent type I signaling, or the IFN-β promoter in combination with mda5 or RIG-I expression plasmids were used. While the wild-type V protein strongly inhibited

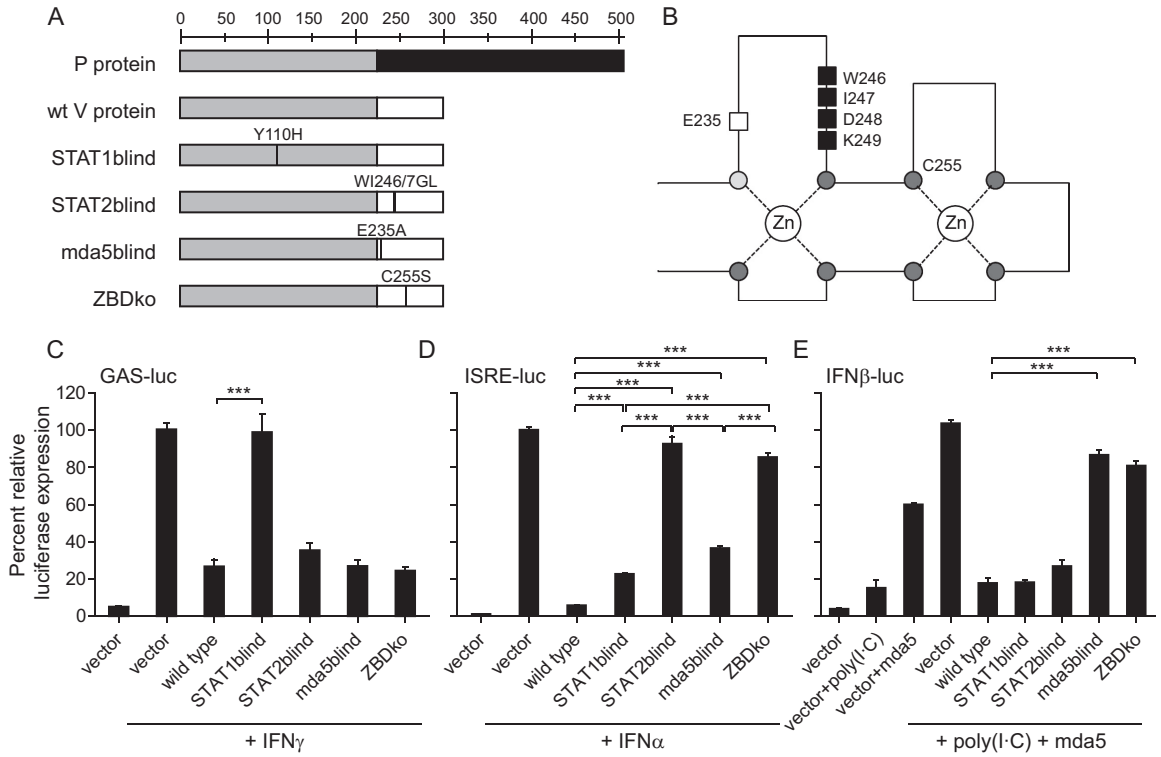

FIG 2 Generation of CDV V-protein mutants unable to interfere with different IFN signaling pathways. (A) Overview of mutations introduced in the P gene to produce V proteins that are unable to interfere with STAT1, STAT2, or mda5 signaling or that have a disrupted zinc-binding domain (ZBDko). The P/V shared domain is shown in light gray, the RNA editing site is indicated by a black line, and the unique regions of the P or V protein are shown in dark gray or white, respectively. wt, wild type.(B) Positions of the respective mutations in the zinc finger structure of the unique V-protein carboxy terminus (adapted from reference 11 with permission of the publisher). Conserved cysteines (dark gray filled circles) and the conserved histidine (light gray filled circle) are indicated. The mda5-interacting residue E235 (white box) and the STAT2-interacting residues (black boxes) are shown. (C to E) IFN signaling interference activity of the V-protein mutants. Huh7 cells were transfected with either a GAS-luciferase reporter plasmid (C) or ISRE-luciferase reporter plasmid (D) or an IFN-β-luciferase reporter gene plasmid (E) together with a mda5 expression plasmid, in combination with either an empty vector, or vectors expressing the CDV wild-type V protein, or the respective mutant CDV V proteins as indicated. Cells were treated with 100 ng/ml of IFN-γ or 1,000 U/ml of IFN-α or transfected with 1 μg/ml of poly(I·C) for 18 h, 8 h, or 20 h prior to lysis, respectively, and luciferase activity was measured. Luciferase activity of cells transfected with an empty vector was set at 100%. Values are the averages of three experiments done in triplicate; error bars indicate the standard errors of the means (SEM). Asterisks show the levels of statistical significance for the values indicated by the ends of the bars (***, $P < 0.001$).

the induction of all these pathways, the respective signaling activity was selectively restored for the STAT1blind, STAT2blind, and mda5blind V protein mutants (Fig. 2C to E). However, in contrast to the type II IFN- and mda5-dependent signaling pathways, which were fully inhibited by all other mutants (Fig. 2C and E), a partial but significant ($P < 0.001$) loss of type I IFN signaling inhibition was also observed for the STAT1blind V protein and even more for the mda5blind V protein. Disruption of the zinc-binding domain in the V-protein carboxy terminus, which is highly conserved among all paramyxoviruses, prevented interference with the STAT2 and mda5 signaling pathways at levels close to the respective individual STAT2blind and mda5blind mutants (Fig. 2D and E). Consistent with previous reports (7), RIG-I overexpression prevented the CDV V-protein-mediated inhibition of IFN-β promoter activation (data not shown).

STAT1blind and STAT2blind CDV V proteins selectively lose their ability to prevent nuclear translocation of the respective STAT protein. Morbillivirus V proteins prevent type I and II IFN signaling by retaining STAT1 and STAT2 in the cytoplasm (16, 28). To evaluate the extent of STAT1 and STAT2 nuclear translocation inhibition associated with the different mutants, the intracellular distribution of the respective proteins was quantified by confocal microscopy after stimulation with IFN-γ and IFN-α, respectively. As reported previously (16), the wild-type CDV V protein efficiently blocked STAT1 and STAT2 nuclear translocation, while the STAT1blind mutant was no longer able to prevent STAT1 translocation (Fig. 3). The STAT2blind mutant no longer affected STAT2 distribution, while the mda5blind and ZBDko mutants retained their ability to block STAT1 and STAT2 nuclear translocation, albeit to a lesser extent than the wild-type CDV V protein (Fig. 4). The complete loss of type I IFN signaling inhibition seen for the ZBDko mutant (Fig. 2D) may thus be due to an additive effect of partial STAT2 cytoplasmic retention and the lack of mda5-mediated signaling (Fig. 2D) associated with this mutant.

Viruses carrying mutant V proteins replicate efficiently in IFN signaling-deficient cells. To evaluate V-protein interference with the different IFN signaling pathways in the viral context, we introduced the respective mutations into the genome of 5804PeH, which expresses eGFP from an additional open reading frame inserted between the H and L genes (24). The Vko virus from a previous study was included as a control for complete loss of V-protein function (22). Western blot analysis revealed that all mutant V proteins were efficiently expressed and that the P-to-V ratios remained around 1:1 (Fig. 5A and data not shown). Time

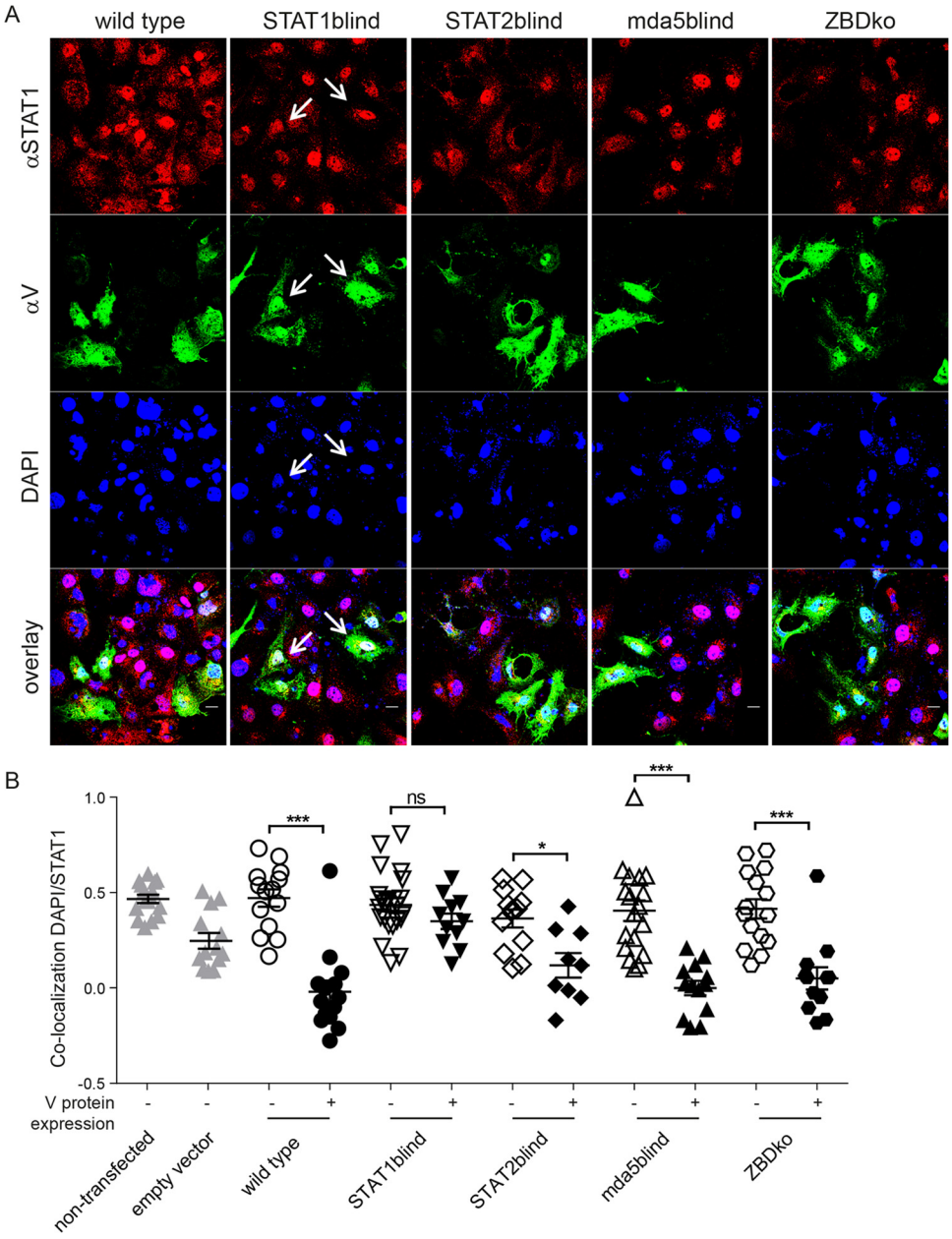

FIG 3 Nuclear translocation of STAT1 in the presence of different V-protein mutants. V-protein-expressing Huh7 cells were treated with 2,000 U/ml IFN-γ for 30 min 36 h posttransfection. The cells were stained with an anti-phospho-STAT1 (αSTAT1) (C-111; Santa Cruz Biotechnology) monoclonal antibody (red) and a rabbit antipeptide hyperimmune serum against the P/V shared region (αV) (green). Nuclei were counterstained with DAPI (blue). (A) Confocal microscopic images at 600-fold magnification are shown. Colocalization is indicated by white arrows. (B) Single-cell analysis of DAPI/STAT1 colocalization after IFN-γ treatment of transfected versus nontransfected cells. Pearson's coefficients were calculated for nontransfected (open symbols) and transfected cells (closed symbols) in the same well. Each symbol represents the value for an individual cell; the mean (black horizontal line) and standard deviation (error bar) for each sample are indicated. Values around 0 indicate random protein distribution, while values above or below 0 represent colocalization or lack thereof, respectively. Nontransfected and vector controls are indicated by gray symbols. Symbols represent cells counted from at least 8 photos of two individual experiments (means ± SEM). The levels of statistical significance by one-way analysis of variance (ANOVA) with Bonferroni's multiple-comparison test are indicated above the bars as follows: *, $P < 0.05$; ***, $P < 0.001$; ns, no significance.

course analysis of cell-associated and cell-free virus production revealed similar replication efficiencies during early infection stages (Fig. 5B and C). While the replication kinetics of the STAT1blind virus were similar to that of the parental wild-type virus throughout, the cell-associated virus titers of the STAT2blind virus and to a lesser extent the mda5blind virus were significantly lower at later time points ($P < 0.05$ to 0.01), even though the cytopathic effects were similar (Fig. 5B and D). These viruses and the Vko and ZBDko mutants also yielded significantly ($P < 0.05$ to 0.001) lower cell-free virus titers at the latest time point (Fig. 5C), suggesting that the V-protein unique region may influence directly or indirectly virus replication. However, the peak titers

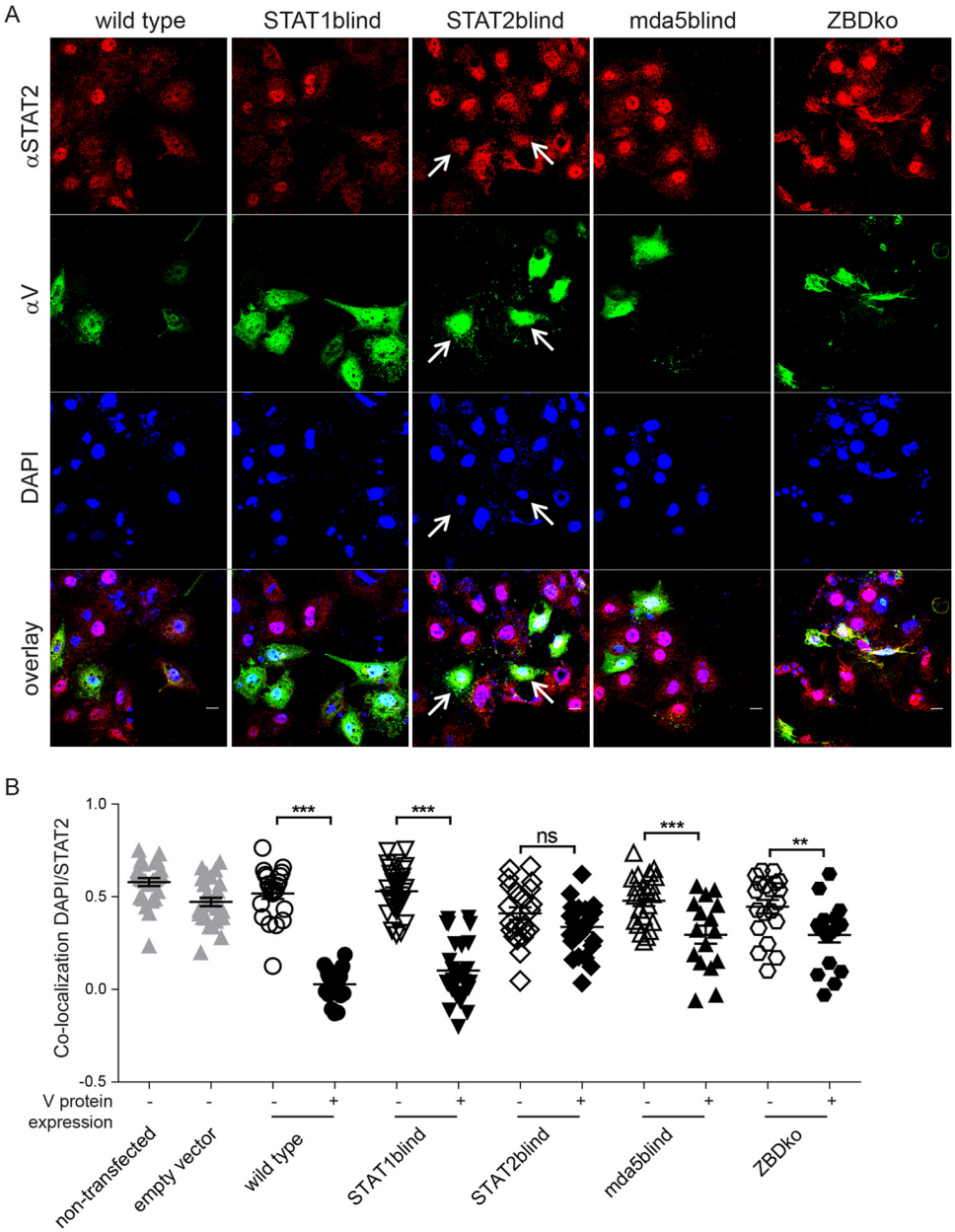

FIG 4 Nuclear translocation of STAT2 in the presence of different V-protein mutants. V-transfected Huh7 cells were treated with 1,000 U/ml IFN-α for 30 min at 36 h posttransfection. The cells were stained with an anti-STAT2 (A-7; Santa Cruz Biotechnology) monoclonal antibody (red) and a rabbit antipeptide hyperimmune serum against the P/V shared region (green). Nuclei were counterstained with DAPI (blue). (A) Confocal microscopic images at 600-fold magnification are shown. Colocalization is indicated by white arrows. (B) Single-cell analysis of DAPI/STAT2 colocalization after IFN-α treatment of transfected versus nontransfected cells. The analysis was performed as described in the legend to Fig. 3.

reached and the overall replication kinetics were within the range observed for different wild-type viruses.

CDV virulence requires inhibition of STAT2 and mda5 signaling. To assess the importance of the V-protein-mediated inhibition of the different IFN signaling pathways *in vivo*, groups of six to eight ferrets were infected intranasally with each mutant virus, the wild-type virus, and the Vko virus. All animals infected with the wild-type or STAT1blind viruses developed a severe rash, high fever, and substantial weight loss and ultimately succumbed to the disease within 2 weeks after infection (Fig. 6A). In contrast, only a mild and transient disease was observed in the groups of ferrets infected with Vko or ZBDko virus. Ferrets infected with mda5blind and STAT2blind viruses presented an intermediate disease phenotype with clinical signs of various intensities. However, all animals ultimately survived the infection. Consistent with the clinical course, cell-associated viremia levels observed for the STAT1blind virus were similar to those observed for the wild-type strain (Fig. 6B). In contrast, all other V-protein mutants reached a hundred-fold-lower peak titer, and the viremia was cleared within 3 weeks. None of the viruses reverted to the wild-type sequence or accumulated additional changes in the region surrounding the original mutation (data not shown).

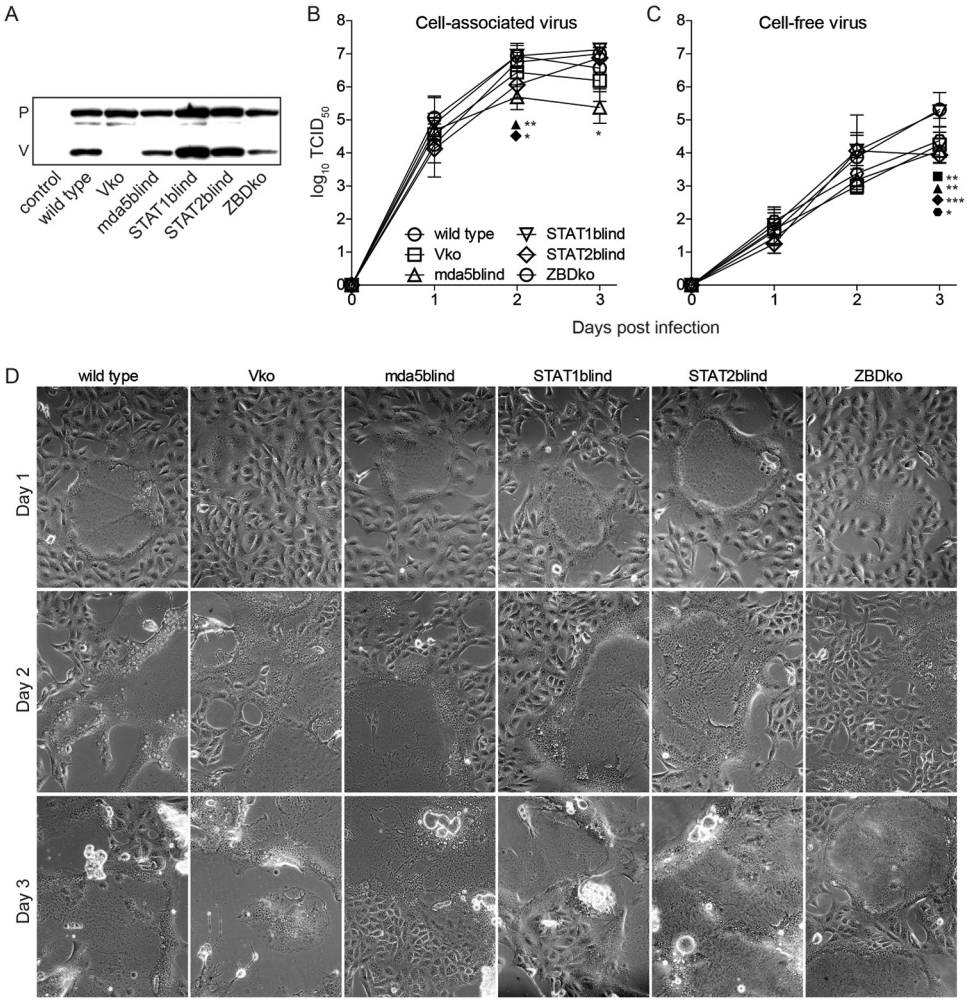

FIG 5 *In vitro* characterization of P/V mutant viruses. (A) Western blot analysis of the P and V proteins expressed by the wild-type strain 5804PeH and the respective IFN signaling blind viruses. V proteins were visualized using a rabbit antipeptide hyperimmune serum against the P/V shared region. (B and C) Growth curve analysis of the respective viruses on VerodogSLAMtag cells at a multiplicity of infection of 0.01. Data points represent averages of cell-associated (B) and cell-free (C) virus titers expressed as 50% tissue culture infectious doses ($TCID_{50}$)/ml. Error bars indicate SEM. Asterisks show the levels of statistical significance as follows: *, $P < 0.05$; **, $P < 0.01$; ***, $P < 0.001$. (D) Cytopathic effect observed at the different time points. Phase-contrast pictures were taken at the time of sample harvest. Specifically, 200-fold magnifications are shown.

All viruses resulted in severe leukopenia within 7 days after infection, which resolved rapidly in animals infected with Vko, mda5/STAT2blind, or STAT2blind viruses, while progressively worsening in animals infected with lethal STAT1blind or wild-type strains (Fig. 6C). Despite the survival of all animals infected with the mda5blind virus, leukocyte numbers remained reduced until the end of this study at 35 days postinfection. Similarly, an inhibition of lymphocyte proliferation was observed in all groups during the acute infection stages, with the exception of the Vko-infected animals (Fig. 6D). The values remained low in the animals infected with the lethal viruses and recovered only slowly in the mda5 and combined STAT2/mda5blind groups. In contrast, lack of interference with STAT2-mediated IFN signaling resulted in a rapid recovery of proliferation activity.

STAT1blind virus remains virulent despite reduced control of type I IFN responses *in vivo*. Lethal CDV infections in ferrets are characterized by complete inhibition of cytokine responses (26). To assess whether the loss of type I and II IFN signaling interference observed *in vitro* alters the IFN induction profile *in vivo*, we analyzed the IFN mRNA levels in PBMCs 3 days after infection. Consistent with our previous findings, ferrets infected with the parental wild-type strain were unable to upregulate type I and II IFN mRNAs, while the group infected with Vko virus mounted a vigorous response (22) (Fig. 7A to C, WT and Vko columns). All viruses that carried V proteins with mutations that selectively abolished their ability to interfere with one of the IFN signaling pathways resulted in an intermediate phenotype (Fig. 7A to C). IFN-γ induction in these animals was less homogeneous, with some animals responding strongly and others showing inhibition similar to that of the group infected with wild-type virus (Fig. 7C). While the STAT1blind mutant retained wild-type virulence despite its reduced ability to prevent IFN induction in PBMCs 3 days postinfection, the STAT2blind, mda5blind, and ZBDko viruses that also had reduced ability to prevent IFN induction were attenuated. This suggests that virus-host interactions in other cells, or downstream IFN signaling events, must influence disease outcome.

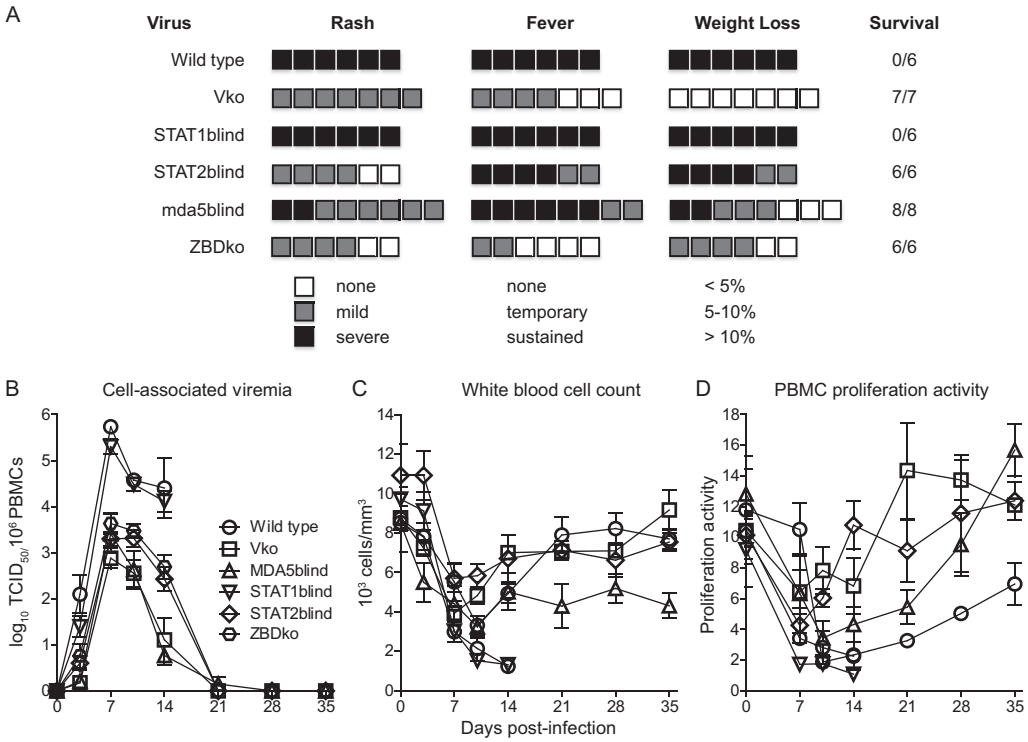

FIG 6 Virulence of P/V mutant viruses. Groups of six to eight animals were inoculated intranasally with 10^5 $TCID_{50}$ of the respective virus and observed for up to 5 weeks. (A) Disease severity. Rash, fever, weight loss, and survival are shown. Each box represents one animal. For rash, black indicates the most severe skin eruption, gray represents a mild rash, and white represents no rash. For fever, black indicates a body temperature above 39.2°C sustained for at least 3 days, gray represents a body temperature of more than 39.2°C sustained not more than 2 days, and white represents normal body temperature between 37.8°C and 39.2°C. For weight loss, black indicates a loss of more than 10% of initial body weight, gray represents a 5 to 10% loss, and white represents a weight loss below 5%. The number of animals euthanized for humane reasons is indicated in the Survival column. (B) Viral load, expressed as number of CDV-infected cells per million PBMC. (C) White blood cell count per microliter of blood. (D) Proliferation activity of PBMCs expressed as a ratio of BrdU incorporation detected in phytohemagglutinin-stimulated and nonstimulated cells. Data points represent the averages of all animals infected, and error bars indicate the SEM.

DISCUSSION

Morbillivirus V-protein-mediated interference with innate immune activation has been the focus of intense study over the last years. It is now clear that V protein inhibits the nuclear translocation of STAT1 and STAT2, thereby interfering with type I and II IFN-mediated transcriptional activation (16, 28, 30). In addition, V protein inhibits mda5 signaling (19). Naturally occurring mutations and systematic screening have identified the region around residue Y110 as essential for STAT1 interactions (6, 14, 31) and have highlighted the importance of regions R233-E235 and W240-W250 in the V-protein unique region for mda5 signaling interference and STAT2 binding, respectively (6, 8). Independent of these *in vitro* mechanistic analyses, the importance of the V protein for virulence has been demonstrated in different animal

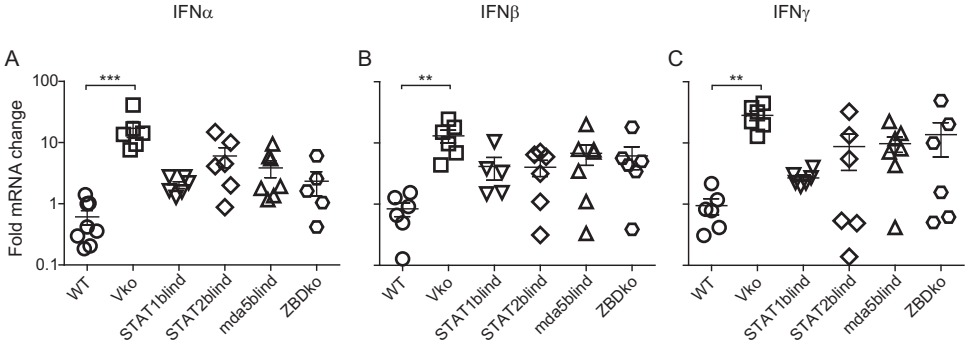

FIG 7 Control of type I and II IFN responses in PBMCs. (A to C) Levels of IFN-α (A), IFN-β (B), andIFN-γ (C) mRNA expression in PBMCs of animals infected with the parental strain 5804PeH (WT), the Vko derivative, or the different mutant viruses. RNA was isolated from PBMCs on day 0 and 3 postinfection, and PCR assays were conducted using primers specific for the genes indicated at the top of each panel (IFN-α, IFN-β, and IFN-γ). The fold change ratios between experimental and control samples for each gene were calculated and normalized against GAPDH using the $\Delta\Delta C_T$ method. Error bars represent the SEM. Asterisks show the levels of statistical significance as follows: **, $P < 0.01$; ***, $P < 0.001$.

models (20, 22, 32), and a STAT1blind virus displayed a Vko phenotype in rhesus macaques (21). However, the relative importance of the V-protein interactions with the different IFN signaling pathways for virulence and innate immune response control remained to be determined. We present here such an analysis based on infection of ferrets with a lethal CDV strain. Surprisingly, we found that loss of the ability to interfere with STAT1 signaling had no effect on the severity of immunosuppression and the outcome of the infection in ferrets, even though this virus was unable to prevent activation of type I and II IFN transcription in PBMCs.

Control of STAT2 and mda5-mediated signaling is critical for morbillivirus virulence. RNA virus infections are first detected by the intracellular RNA sensors RIG-I and mda5, triggering the transcription of IFN-β, which in turn initiates a signaling cascade that ultimately leads to phosphorylation of tyrosine residues in STAT molecules and their nuclear translocation (33). The best-characterized IFN signaling pathway involves the binding of phosphorylated STAT1/2 molecules to interferon regulatory factor 9 (IRF9), which leads to the formation of interferon-stimulated gene factor 3 (ISGF3) and subsequent transcription of ISRE-controlled genes (34). In addition, other mechanisms of signaling exist, and there is increasing evidence that STAT1, STAT3, STAT4, STAT5, and STAT6 homodimers, as well as STAT1/3, STAT1/4, STAT1/5, STAT2/3 and STAT5/6 heterodimers also engage in signal transduction (35, 36). Furthermore, interferon-stimulated genes (ISGs) cannot be induced upon stimulation with IFN in an ISRE-dependent manner in the presence of p38 inhibitors (37), indicating that STAT-independent signaling via p38 and mitogen-activated protein kinases (MAPK) contributes significantly to IFN-mediated transcription initiation (35). Altogether, these *in vitro* and knockout mouse studies suggest that several different pathways of interferon signaling are operative, but it is not yet known which are more relevant for the control of virulence in natural hosts. We observed that functional inactivation of V-protein-meditated inhibition of STAT2- or mda5-mediated signaling results in attenuation, demonstrating that interference at several key points in the innate immune recognition pathway is necessary for the virus to achieve full control.

Minor role of STAT1 signaling in host response to CDV. The increased susceptibility of STAT1ko mice, and of patients with genetic defects in STAT1, to many viral diseases illustrates its importance in the activation of the host response to infections (38, 39). Together with an earlier report that MeV inhibits the maturation of SLAM-expressing STAT2ko but not STAT1ko murine dendritic cells (40), our observation that the inhibition of STAT1-mediated signaling has little effect on CDV virulence in ferrets indicates that the STAT1 signaling pathway plays only a minor role in the control of these infections in a natural host. However, a similarly constructed STAT1blind measles virus was attenuated in rhesus macaques (21). The relative importance of the interactions of the V proteins of morbilliviruses with the immune defenses of different hosts may thus vary.

V-protein interference with additional signaling or effector proteins and disease severity. We observed that all viruses with IFN signaling interference-deficient V proteins partially lost their competence to control IFN activation in ferret PBMCs, but only the STAT1blind CDV retained wild-type virus-like virulence. It is conceivable that early CDV interactions with macrophages and dendritic cells of the respiratory tract determine disease outcome, as these cells were found to be infected during early MeV infection stages (41). These professional antigen-presenting cells rapidly express high levels of type I IFNs upon exposure of Toll-like receptors to single-stranded RNA (42). The MeV V protein inhibits this pathway by competing with IRF7 for phosphorylation (43), and high structural and functional conservation suggests that the CDV V protein has similar activity.

Differences in the interference of the mutants with downstream IFN signaling may also contribute to disease outcome. While small amounts of type I or II IFN can be sufficient to trigger the expression of ISGs (33), there are several positive- and negative-feedback loops to adapt the level of expression to the respective situation (44, 45). It is conceivable that V protein interacts with certain groups of ISGs in a yet unknown manner and that these interactions may modulate virulence. Identification and characterization of these candidate additional V-protein targets may thus be needed to fully understand the multifaceted interaction between morbilliviruses and the host's immune system.

ACKNOWLEDGMENTS

The p125-Luc plasmid was a kind gift of Georg Kochs at the Institute for Medical Microbiology and Hygiene, University of Freiburg, Germany, and the mda5 and RIG-I expression plasmids were generously provided by Manoj Krishnan at the Duke-NUS Graduate Medical School. We thank all laboratory members for continuing support and lively discussions.

This work was supported by CIHR grant MOP66989, funding from the German Ministry of Health, and a Duke-NUS Signature Research Program start-up grant (funded by the Agency for Science, Technology and Research of Singapore and the Ministry of Health of Singapore) to V.V.M., NIH grant R01 AI063476 to R.C., Armand-Frappier Foundation fellowships to N.S. and C.G., a postdoctoral fellowship by the German Research Foundation (DFG; GE2325/1-1) to I.G., funding from the Helmholtz-Alberta Initiative-Infectious Diseases Research (HAI-IDR) to E.G., and funding from the Helmholtz Virtual Institute VISTRIE (Viral Strategies of Immune Evasion) to M.D.

REFERENCES

1. **Schneider-Schaulies S, Schneider-Schaulies J.** 2009. Measles virus-induced immunosuppression. Curr. Top. Microbiol. Immunol. **330:**243–269.
2. **von Pirquet CE.** 1908. Das Verhalten der kutanen Tuberkulinreaktion während der Masern. Dtsch. Med. Wochenschr. **30:**1297–1300.
3. **Moss WJ, Griffin DE.** 2006. Global measles elimination. Nat. Rev. Microbiol. **4:**900–908. http://dx.doi.org/10.1038/nrmicro1550.
4. **Abramson O, Dagan R, Tal A, Sofer S.** 1995. Severe complications of measles requiring intensive care in infants and young children. Arch. Pediatr. Adolesc. Med. **149:**1237–1240. http://dx.doi.org/10.1001/archpedi.1995.02170240055008.
5. **Dollimore N, Cutts F, Binka FN, Ross DA, Morris SS, Smith PG.** 1997. Measles incidence, case fatality, and delayed mortality in children with or without vitamin A supplementation in rural Ghana. Am. J. Epidemiol. **146:**646–654. http://dx.doi.org/10.1093/oxfordjournals.aje.a009330.
6. **Caignard G, Bourai M, Jacob Y, Tangy F, Vidalain PO.** 2009. Inhibition of IFN-alpha/beta signaling by two discrete peptides within measles virus V protein that specifically bind STAT1 and STAT2. Virology **383:**112–120. http://dx.doi.org/10.1016/j.virol.2008.10.014.
7. **Childs K, Stock N, Ross C, Andrejeva J, Hilton L, Skinner M, Randall R, Goodbourn S.** 2007. mda-5, but not RIG-I, is a common target for paramyxovirus V proteins. Virology **359:**190–200. http://dx.doi.org/10.1016/j.virol.2006.09.023.
8. **Ramachandran A, Parisien JP, Horvath CM.** 2008. STAT2 is a primary target for measles virus V protein-mediated alpha/beta interferon signaling inhibition. J. Virol. **82:**8330–8338. http://dx.doi.org/10.1128/JVI.00831-08.
9. **Thomas SM, Lamb RA, Paterson RG.** 1988. Two mRNAs that differ by two nontemplated nucleotides encode the amino coterminal proteins P and V of the paramyxovirus SV5. Cell **54:**891–902. http://dx.doi.org/10.1016/S0092-8674(88)91285-8.

10. **Cattaneo R, Kaelin K, Baczko K, Billeter MA.** 1989. Measles virus editing provides an additional cysteine-rich protein. Cell **56:**759–764. http://dx.doi.org/10.1016/0092-8674(89)90679-X.
11. **Li T, Chen X, Garbutt KC, Zhou P, Zheng N.** 2006. Structure of DDB1 in complex with a paramyxovirus V protein: viral hijack of a propeller cluster in ubiquitin ligase. Cell **124:**105–117. http://dx.doi.org/10.1016/j.cell.2005.10.033.
12. **Paterson RG, Leser GP, Shaughnessy MA, Lamb RA.** 1995. The paramyxovirus SV5 V protein binds two atoms of zinc and is a structural component of virions. Virology **208:**121–131. http://dx.doi.org/10.1006/viro.1995.1135.
13. **Lamb RA, Parks GD.** 2013. Paramyxoviridae: the viruses and their replication, p 957–995. *In* Knipe DM, Howley PM (ed), Fields virology, 6th ed. Lippincott Williams & Wilkins, Philadelphia, PA.
14. **Ohno S, Ono N, Takeda M, Takeuchi K, Yanagi Y.** 2004. Dissection of measles virus V protein in relation to its ability to block alpha/beta interferon signal transduction. J. Gen. Virol. **85:**2991–2999. http://dx.doi.org/10.1099/vir.0.80308-0.
15. **Devaux P, von Messling V, Songsungthong W, Springfeld C, Cattaneo R.** 2007. Tyrosine 110 in the measles virus phosphoprotein is required to block STAT1 phosphorylation. Virology **360:**72–83. http://dx.doi.org/10.1016/j.virol.2006.09.049.
16. **Rothlisberger A, Wiener D, Schweizer M, Peterhans E, Zurbriggen A, Plattet P.** 2010. Two domains of the V protein of virulent canine distemper virus selectively inhibit STAT1 and STAT2 nuclear import. J. Virol. **84:**6328–6343. http://dx.doi.org/10.1128/JVI.01878-09.
17. **Andrejeva J, Childs KS, Young DF, Carlos TS, Stock N, Goodbourn S, Randall RE.** 2004. The V proteins of paramyxoviruses bind the IFN-inducible RNA helicase, mda-5, and inhibit its activation of the IFN-beta promoter. Proc. Natl. Acad. Sci. U. S. A. **101:**17264–17269. http://dx.doi.org/10.1073/pnas.0407639101.
18. **Childs KS, Andrejeva J, Randall RE, Goodbourn S.** 2009. Mechanism of mda-5 inhibition by paramyxovirus V proteins. J. Virol. **83:**1465–1473. http://dx.doi.org/10.1128/JVI.01768-08.
19. **Ramachandran A, Horvath CM.** 2010. Dissociation of paramyxovirus interferon evasion activities: universal and virus-specific requirements for conserved V protein amino acids in MDA5 interference. J. Virol. **84:**11152–11163. http://dx.doi.org/10.1128/JVI.01375-10.
20. **Devaux P, Hodge G, McChesney MB, Cattaneo R.** 2008. Attenuation of V- or C-defective measles viruses: infection control by the inflammatory and interferon responses of rhesus monkeys. J. Virol. **82:**5359–5367. http://dx.doi.org/10.1128/JVI.00169-08.
21. **Devaux P, Hudacek AW, Hodge G, Reyes-Del Valle J, McChesney MB, Cattaneo R.** 2011. A recombinant measles virus unable to antagonize STAT1 function cannot control inflammation and is attenuated in rhesus monkeys. J. Virol. **85:**348–356. http://dx.doi.org/10.1128/JVI.00802-10.
22. **von Messling V, Svitek N, Cattaneo R.** 2006. Receptor (SLAM [CD150]) recognition and the V protein sustain swift lymphocyte-based invasion of mucosal tissue and lymphatic organs by a morbillivirus. J. Virol. **80:**6084–6092. http://dx.doi.org/10.1128/JVI.00357-06.
23. **von Messling V, Springfeld C, Devaux P, Cattaneo R.** 2003. A ferret model of canine distemper virus virulence and immunosuppression. J. Virol. **77:**12579–12591. http://dx.doi.org/10.1128/JVI.77.23.12579-12591.2003.
24. **von Messling V, Milosevic D, Cattaneo R.** 2004. Tropism illuminated: lymphocyte-based pathways blazed by lethal morbillivirus through the host immune system. Proc. Natl. Acad. Sci. U. S. A. **101:**14216–14221. http://dx.doi.org/10.1073/pnas.0403597101.
25. **Anderson DE, von Messling V.** 2008. Region between the canine distemper virus M and F genes modulates virulence by controlling fusion protein expression. J. Virol. **82:**10510–10518. http://dx.doi.org/10.1128/JVI.01419-08.
26. **Svitek N, von Messling V.** 2007. Early cytokine mRNA expression profiles predict Morbillivirus disease outcome in ferrets. Virology **362:**404–410. http://dx.doi.org/10.1016/j.virol.2007.01.002.
27. **Schmittgen TD, Zakrajsek BA, Mills AG, Gorn V, Singer MJ, Reed MW.** 2000. Quantitative reverse transcription-polymerase chain reaction to study mRNA decay: comparison of endpoint and real-time methods. Anal. Biochem. **285:**194–204. http://dx.doi.org/10.1006/abio.2000.4753.
28. **Palosaari H, Parisien JP, Rodriguez JJ, Ulane CM, Horvath CM.** 2003. STAT protein interference and suppression of cytokine signal transduction by measles virus V protein. J. Virol. **77:**7635–7644. http://dx.doi.org/10.1128/JVI.77.13.7635-7644.2003.
29. **Parisien JP, Bamming D, Komuro A, Ramachandran A, Rodriguez JJ, Barber G, Wojahn RD, Horvath CM.** 2009. A shared interface mediates paramyxovirus interference with antiviral RNA helicases MDA5 and LGP2. J. Virol. **83:**7252–7260. http://dx.doi.org/10.1128/JVI.00153-09.
30. **Chinnakannan SK, Nanda SK, Baron MD.** 2013. Morbillivirus V proteins exhibit multiple mechanisms to block type 1 and type 2 interferon signalling pathways. PLoS One **8:**e57063. http://dx.doi.org/10.1371/journal.pone.0057063.
31. **Bankamp B, Fontana JM, Bellini WJ, Rota PA.** 2008. Adaptation to cell culture induces functional differences in measles virus proteins. Virol. J. **5:**129. http://dx.doi.org/10.1186/1743-422X-5-129.
32. **Valsamakis A, Schneider H, Auwaerter PG, Kaneshima H, Billeter MA, Griffin DE.** 1998. Recombinant measles viruses with mutations in the C, V, or F gene have altered growth phenotypes in vivo. J. Virol. **72:**7754–7761.
33. **Haller O, Kochs G, Weber F.** 2006. The interferon response circuit: induction and suppression by pathogenic viruses. Virology **344:**119–130. http://dx.doi.org/10.1016/j.virol.2005.09.024.
34. **van Boxel-Dezaire AH, Rani MR, Stark GR.** 2006. Complex modulation of cell type-specific signaling in response to type I interferons. Immunity **25:**361–372. http://dx.doi.org/10.1016/j.immuni.2006.08.014.
35. **Platanias LC.** 2005. Mechanisms of type-I- and type-II-interferon-mediated signalling. Nat. Rev. Immunol. **5:**375–386. http://dx.doi.org/10.1038/nri1604.
36. **Kallal LE, Biron CA.** 2013. Changing partners at the dance: variations in STAT concentrations for shaping cytokine function and immune responses to viral infections. JAKSTAT **2**(1):e23504. http://dx.doi.org/10.4161/jkst.23504.
37. **Uddin S, Majchrzak B, Woodson J, Arunkumar P, Alsayed Y, Pine R, Young PR, Fish EN, Platanias LC.** 1999. Activation of the p38 mitogen-activated protein kinase by type I interferons. J. Biol. Chem. **274:**30127–30131. http://dx.doi.org/10.1074/jbc.274.42.30127.
38. **Najjar I, Fagard R.** 2010. STAT1 and pathogens, not a friendly relationship. Biochimie **92:**425–444. http://dx.doi.org/10.1016/j.biochi.2010.02.009.
39. **Boisson-Dupuis S, Kong XF, Okada S, Cypowyj S, Puel A, Abel L, Casanova JL.** 2012. Inborn errors of human STAT1: allelic heterogeneity governs the diversity of immunological and infectious phenotypes. Curr. Opin. Immunol. **24:**364–378. http://dx.doi.org/10.1016/j.coi.2012.04.011.
40. **Hahm B, Trifilo MJ, Zuniga EI, Oldstone MB.** 2005. Viruses evade the immune system through type I interferon-mediated STAT2-dependent, but STAT1-independent, signaling. Immunity **22:**247–257. http://dx.doi.org/10.1016/j.immuni.2005.01.005.
41. **Lemon K, de Vries RD, Mesman AW, McQuaid S, van Amerongen G, Yuksel S, Ludlow M, Rennick LJ, Kuiken T, Rima BK, Geijtenbeek TB, Osterhaus AD, Duprex WP, de Swart RL.** 2011. Early target cells of measles virus after aerosol infection of non-human primates. PLoS Pathog. **7:**e1001263. http://dx.doi.org/10.1371/journal.ppat.1001263.
42. **Bao M, Liu YJ.** 2013. Regulation of TLR7/9 signaling in plasmacytoid dendritic cells. Protein Cell **4:**40–52. http://dx.doi.org/10.1007/s13238-012-2104-8.
43. **Pfaller CK, Conzelmann KK.** 2008. Measles virus V protein is a decoy substrate for IkappaB kinase alpha and prevents Toll-like receptor 7/9-mediated interferon induction. J. Virol. **82:**12365–12373. http://dx.doi.org/10.1128/JVI.01321-08.
44. **Marié I, Durbin JE, Levy DE.** 1998. Differential viral induction of distinct interferon-alpha genes by positive feedback through interferon regulatory factor-7. EMBO J. **17:**6660–6669. http://dx.doi.org/10.1093/emboj/17.22.6660.
45. **Sato M, Hata N, Asagiri M, Nakaya T, Taniguchi T, Tanaka N.** 1998. Positive feedback regulation of type I IFN genes by the IFN-inducible transcription factor IRF-7. FEBS Lett. **441:**106–110. http://dx.doi.org/10.1016/S0014-5793(98)01514-2.